UAV Autonomous Indoor Exploration and Mapping for SAR Missions: Reflections from the ICUAS 2022 Competition*

Adil Farooq[1,2], Antreas Anastasiou[1,2], Nicolas Souli[1,2], Christos Laoudias[1], Panayiotis S. Kolios[1], and Theocharis Theocharides[1,2]

***Abstract*— The technological advancement in Unmanned Aerial Vehicles (UAVs) or drones and their deployment in real-life Search and Rescue (SAR) missions is imminent. We, therefore, present a perception-aware autonomous exploration framework aimed at performing vision-based target detection and collision avoidance with an Unmanned Aerial Vehicle (UAV). The UAV utilizes a depth camera for maneuvering and finding the target. The underlying indoor exploration approach considers autonomous collision-free navigation, as well as target detection with a ballistic ball payload delivery without a prior map. Moreover, the proposed method allows safe navigation in enclosed unknown areas congested with randomly positioned obstacles and target locations. Our underlined end-to-end system architecture integrates the proposed exploration strategy. Extensive simulation experiments, using several Key Performance Indicators (KPIs), showcase the effectiveness of the proposed Robot Operating System (ROS) framework in a simulated Gazebo environment under various parameter settings.**

I. Introduction

UAVs are playing a pivotal role in many emergency response applications due to their rapid deployment and ability to reach dangerous and human inaccessible locations. UAVs can be employed in real-time to aid the first responders during SAR missions [1], e.g., in hazardous environments such as fire incidents [2], [3] or a collapsed building [4], UAVs can be deployed to locate victims or survivors [5]. Despite the UAV technological advancements, in terms of exploration and reliability, those systems are most often controlled by a trained operator to avoid obstructions on such incident sites [6]. For autonomous exploration, the UAVs deployed in SAR missions operate at higher altitudes, with reliable Global Positioning System (GPS) coverage, and no occlusion in their Field of View (FoV). The challenge lies in indoor autonomous exploration for performing rapid deployment, as well as precise localization and mapping in unknown environments using only the onboard perception sensors, e.g., Light Detection And Ranging (LiDAR) or depth (RGB-D) camera.

Existing works in autonomous UAV exploration missions focus on a target-oriented approach to recognize objects of interest in an unknown environment and reach them efficiently [7], [8]. To emulate real-life SAR missions and allow comparative assessment of competing solutions under challenging conditions, several events were organized in the past [9], including the 2020 Mohamed Bin Zayed International Robotics Challenge[1] (MBZIRC) wherein multiple challenges were held, especially the challenge 3 targeted an urban firefighting scenario for cooperated aerial and ground vehicles to navigate, detect, approach, and extinguish multiple simulated fires around and inside a building [10]. Another was the DARPA Subterranean (SubT) Challenge[2] based on extreme conditions in underground environments: human-made tunnels, the urban underground, and natural caves, to perform challenging autonomous exploration missions [11]. Very recently at International Conference on Unmanned Aircraft Systems (ICUAS) 2022, a UAV Competition[3] was organized for the first time, that focused on three main challenges, i.e., exploration, target detection, and precise delivery, that fire fighting UAVs face in a time-constrained urban environment.

UAVs are becoming highly capable of achieving more complex tasks forming dynamic coalition [12] and can plan collision-free planning, to aid the first responders in unknown 3D world environments [13]. The key functionality is the ability to make intelligent decisions for collision-free navigation to reach the targets. For instance, a small UAV can assist the first responders in narrow, congested environments like in caves [14], mines, and tunnels [15]. These decisions are typically based on criteria such as mobility, type of perception sensor, or any other application-specific requirements. The authors in [16] addressed the two pioneering aspects of autonomous exploration i.e., gathering information of the environment and avoiding obstacles while constructing the local map. This was achieved by performing self-position estimation and mapping to generate collision-free trajectories. An onboard LiDAR or a depth camera can be used to detect nearby obstructions around the UAV. A cost function penalizes the proximity to the nearest obstacle and re-plans the flight trajectory in real-time while navigating to the target location. In general, navigation algorithms operate under the assumption that the UAV is capable of collecting data from LiDAR or RGB-D camera sensors to map the unknown environment and plan collision-free paths to the

*This work has been supported by the European Union's Horizon 2020 research and innovation programme under grant agreement No 739551 (KIOS CoE) and from the Republic of Cyprus through the Deputy Ministry of Research, Innovation and Digital Policy and from the Cyprus Research and Innovation Foundation under Grant Agreement EXCELLENCE/0421/0586.

[1]KIOS Research and Innovation Center of Excellence, University of Cyprus, Nicosia, Cyprus

[2]Department of Electrical and Computer Engineering, University of Cyprus, Nicosia, Cyprus

[1]https://www.mbzirc.com/

[2]https://subtchallenge.world/home

[3]ICUAS 2022 UAV Competition, https://bit.ly/3t5oo7V

target, solely through onboard sensing and control units.

In this work, we consider the following real-life SAR mission, yet very challenging. An emergency occurs inside a building, e.g., a fire breaks out and the first responders need to take action to minimize human casualties. The indoor environment is partly or completely *unknown*, or it may no longer reflect the interior of the building, e.g., walls and/or ceilings are collapsing, objects are falling, etc. In this case, the first response team requires an *accurate* indoor map in *short time* before entering the building to operate. Thus, an autonomous UAV system with limited battery life (e.g., typically around 30-35 minutes) needs to be rapidly deployed to swiftly explore and map the unknown space under tight time constraints. UAVs using 3D exploration strategies may perform exceptionally well when there are no limitations; however, their increased complexity and computational overhead reduces considerably the exploration in practice, consequently leading to incomplete maps and unexplored areas. To mitigate the 3D plane uncertainty in a 2D approach, it is possible to maneuver the UAV at a certain altitude above the ground plane such that only obstructions can be viewed in the FoV of the perception sensor [17]. We adopt this approach and present a complete UAV system architecture in Section II. Henceforth, we are interested in the applicability and performance of a 2D exploration strategy on an autonomous UAV platform. To this end, the contributions of this work are:

- We have put forward an exploration strategy for a UAV in completely unknown indoor environments, i.e. without any prior surrounding information, by incorporating collision avoidance, target detection and payload delivery sub-modules while constructing a local 2D floor/occupancy map in Section II.
- We have also included a battery consumption plugin, taken from our previous work [18], to reliably estimate the remaining battery life due to the UAV rotors' mobility; see Section IV-A.2 and use it as a critical performance indicator benchmark.
- We used ROS-Gazebo simulation environment to conduct extensive evaluations for our proposed above-mentioned strategy in a number of challenging environments and analyze the experimental results in Section IV-B. We consider four diverse indoor environments of same size with varying settings (i.e., different entry points for the UAV and target locations).

The rest of the paper is structured as follows. The architecture of the UAV system for autonomous exploration to aid SAR missions is detailed in Section II. Section III overviews the UAV and test-bed simulation setup. The experimental results of our performance evaluation in diverse simulated indoor environments are presented in Section IV. Finally, Section V provides concluding remarks and directions for future work.

II. UAV System Architecture

There are several sub-systems comprising a UAV platform for autonomous exploration, namely *Simultaneous Localization and Mapping (SLAM)* indicated as the inner dashed line, *Controller*, *Trajectory Generation*, *Collision Avoidance*, and *Target Detection* as shown in Fig. 1. In this architecture, ρ denotes the point cloud obtained from depth images converted to laser scans, M represents the explored map of the environment, x' is the current pose estimate, x is the current trajectory generated by the controller, T is the next forward waypoint, and T_R is the reconstructed waypoint to reach the goal.

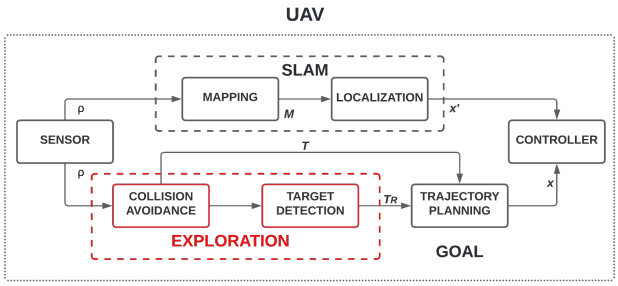

Fig. 1. UAV system architecture for indoor exploration.

Our study entails the development of all these sub-modules that constitute the building foundation for autonomous exploration. The red dotted line in Fig. 1 depicts our main contribution to the collision-free navigation and target detection. Our implemented packages are open-sourced namely, *nav_explorer* and *quadcopter_laser_map* available online[4].

A. Simultaneous Localization and Mapping

An autonomous UAV for indoor exploration in GPS-denied environments requires SLAM to ascertain its location in the unknown environment and gather the sensor data to construct the map. In our solution, we have adopted the grid-based 2D SLAM [19] referred to as GMapping[5], which constructs the occupancy grid/floor maps from laser data. It incorporates a Rao-Blackwellized particle filter SLAM approach to update the map while keeping a minimum number of particles. This leads to a reduction in uncertainty of a robot's pose, position, and orientation on the explored map.

B. Controller

The controller sub-system uses a Software-In-The-Loop (SITL) approach to simulate low-level flight controllers. The simulation stack runs on Ardupilot[6], which enables an easier transition from simulation to a real UAV platform. The controller itself is a set of cascaded PID controllers taken from the open-source *uav_ros_stack* package[7], whose parameters are set to get a desirable response during hovering and while performing complex maneuvers.

[4] https://github.com/aanast01?tab=repositories
[5] http://wiki.ros.org/gmapping
[6] https://ardupilot.org/
[7] https://github.com/larics/uav_ros_stack

C. Trajectory Planning

In the trajectory planning, next waypoints are sent to a Time-Optimal Path Parameterization Based on Reachability Analysis (TOPP-RA) algorithm [20] that interpolates a trajectory between current UAV pose and the target waypoint. The position controller of the UAV receives the given sampled path trajectory in form of waypoints as a reference and commands the UAV rotor.

D. Collision Avoidance

The main part of the exploration was to autonomously navigate in the indoor environment without colliding with the obstructions while constructing a 2D occupancy/floor map. For the UAV to find the way through different positioned obstructions in $\mathcal{E}_i,\ i = 1, \ldots, 4$, given in Table I, we had developed a collision avoidance algorithm, which can safely navigate using the laser scan data extracted from the converted depth images received from the camera, as mentioned in Section II. The pseudocode for our approach is shown in Algorithm 1.

Algorithm 1 Collision Avoidance

Require: $laser\_scans \leftarrow depth\_images$
Ensure: $regions[left, front, right]$
  while $flag = start$ **do**
    if front is clear **then**
      go_front
    else if $left\_obst \leq right\_obst$ **then**
      go_left
    else
      go_right
    end if
    $new\_waypoints[x, y, z] \leftarrow velocities$
  end while

Where the algorithm requires laser scans to construct three regions of the FOV namely, the left, front, and right regions. If there are no obstructions in the center of the view, the UAV moves in front otherwise it compares the number of obstructions between both left and right regions. Given priority to the left region, if there are fewer obstructions it moves to the left side else it moves to the right side. Once the front region is obstruction-free, velocities are given to move to the next forward generated way-points. A threshold to detect the obstructions using the laser scans was set to $1.80\,\mathrm{m}$.

E. Target Detection and Payload Delivery

We find the target pose, i.e., the location of the ARTag from the actual position in the world coordinates from an RGB-D camera using the image frames. For this, we used an image processing open-source ROS tracking library named *ar_track_alvar3*[8] to estimate the orientation and position of the detected ARTag marker [21]. The library computes the projective transformations between the camera frame and ARTAg position and outputs the estimated pose. The *ar_track_alvar* package uses the detected corner points to extract a patch of point clouds containing the ARTag and computes its centroid. Then the pose is estimated by aligning the centroid with the center of the ARTag.

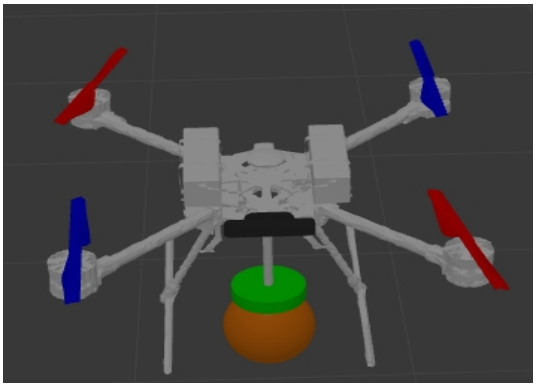

Fig. 2. Kopterworrx Eagle with a ball payload.

To complete the mission, the UAV needed to explore the environment and search for the target i.e. the fire marked as an ARTag (a unique fiducial marker). When the target is detected, the pose in the world frame is reconstructed along with an annotated image and published to predefined ROS topics. The reconstructed pose was evaluated for precision to the ground truth of the ARTag in the world frame. Once the UAV finds the target, i.e. the ARTag, it planned a ballistic launch trajectory taking into account the payload i.e., the ball motion model and gravity to launch the fire extinguishing ball to the target.

III. Simulation Setup

Our UAV system was developed following the architecture in Section II and implemented as a docker container[9] in Ubuntu 20.04.4 LTS (Focal Fossa) operating system in ROS Noetic. All simulations were performed on an Intel Core i5-8400 (6 Cores) CPU system operating at 2.80GHz with 16GB of RAM.

A. UAV platform

The UAV is a four-rotor quadcopter modeled after a Kopterworrx Eagle platform shown in Fig. 2, a custom-designed simulation platform used by LARICS team [22]. An *Inertial Measurement Unit (IMU)*, a *depth camera*, *openni_kinect* and *odometry* plugins are placed on the UAV.

B. Test-bed Environment

The firefighting capabilities of UAVs were tested in an enclosed environment of dimensions $16\,\mathrm{m} \times 26\,\mathrm{m}$ partitioned with three zones, as shown in Fig. 3 (left). Zone 1 (shaded in green color) is the start and take-off zone, which is clear from obstructions. Zone 2 (shaded in yellow color) is the exploration and mapping zone having multiple static obstructions. And last, Zone 3 (shaded in blue color) is the

[8] http://wiki.ros.org/ar_track_alvar

[9] https://github.com/larics/icuas22_competition

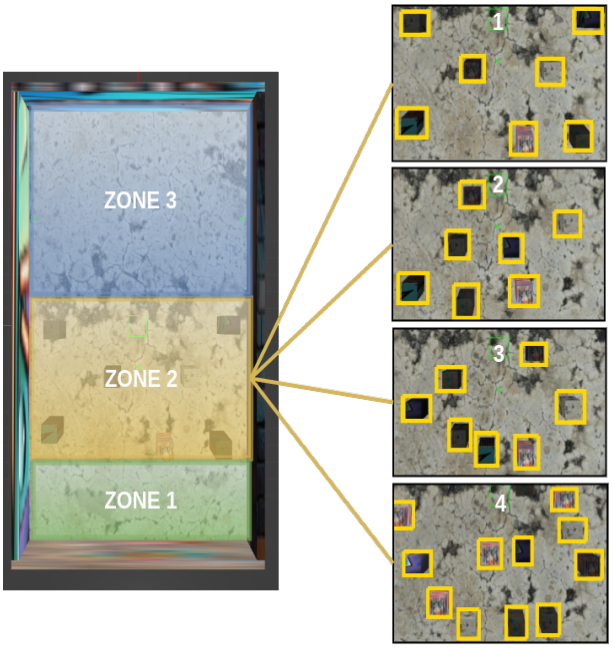

Fig. 3. Test-bed environment with varying obstructions in zone 2.

target detection and ball launch area, and it is obstruction-free.

For our simulation experiments, we selected four challenging indoor environments denoted $\mathcal{E}_i,\ i = 1, \ldots, 4$, listed in Table I, with the varying number of obstructions in Zone 2. Even though there are 7 obstructions in $\mathcal{E}_i,\ i = 1, \ldots, 3$, the locations of the obstructions change, thus increasing the path traversing difficulty level with a narrow opening and dead-ends, as marked 1, 2, and 3 in Fig. 3 (right).

TABLE I
TEST-BED ENVIRONMENT SETUP

Environment	No. of Obstructions	Complexity
$\mathcal{E}_1$	7	Easy
$\mathcal{E}_2$	7	Moderate
$\mathcal{E}_3$	7	Difficult
$\mathcal{E}_4$	11	Very Difficult

IV. PERFORMANCE EVALUATION

We evaluate the performance of our proposed approach described in Section II with respect to a number of KPIs. These include the exploration cost (E_c), battery consumption (B_c), target reconstruction error (R_e), delivery accuracy (D_a), total time (T_t), average speed (S_a), and successful missions (M_s) that are described in the following.

A. Performance Indicators

1) Exploration Cost: The exploration cost E_c is defined as the total distance of the path traversed by the UAV during the exploration mission and is given by [23]

$$E_c = \sum_{i=1}^{n} d_i, \tag{1}$$

where d_i is the length of the path segment i in meters and n is the number of piecewise linear segments that comprise the path.

2) Battery Consumption: We consider battery life a critical performance indicator during autonomous exploration, thus we incorporate a representative battery consumption model. The characteristics of the battery follow a dynamic linear model[10], which we integrate from our previous work [18].

3) Target Reconstruction Error: The given criteria are underlined in the ICUAS 2022 UAV competition rules[11] for determining the accuracy of the reconstructed location of the target. To this end, we define the target reconstruction error R_e as the deviation, i.e., Euclidean distance in meters, between the true and the estimated target positions given by

$$R_e = \sqrt{(x_T - \hat{x}_T)^2 + (y_T - \hat{y}_T)^2 + (z_T - \hat{z}_T)^2}, \tag{2}$$

where $p_T = (x_T, y_T, z_T)$ and $\hat{p}_T = (\hat{x}_T, \hat{y}_T, \hat{z}_T)$ are the true and estimated 3D target positions, respectively. The maximum distance observed to detect the ARTag properly was approximately $4\,\mathrm{m}$.

4) Delivery Accuracy: Similarly, we define the delivery accuracy D_a as the minimum distance in meters between the ball and the target, i.e., the ARTAg, calculated from the moment the ball was launched until it hit the floor. The true target position and the position of the ball delivered by the UAV given by

$$D_a = \min_{p_B} \sqrt{(x_T - x_B)^2 + (y_T - y_B)^2 + (z_T - z_B)^2}, \tag{3}$$

where $p_B = (x_B, y_B, z_B)$ is the 3D ball position.

5) Total Time: The exploration time T_t is defined as the total time elapsed in seconds from the start of the mission until the ball is launched to the detected target. An effective exploration strategy minimizes T_t, while making the UAV maneuver to different locations that maximize the discovered area.

6) Average Speed: The average speed S_a is defined as the total explored distance divided by the total time for the complete mission. To have a better exploration and higher accuracy, an average speed of $0.5\,\mathrm{m/s}$ is optimal.

7) Successful Missions: The UAV system architecture in Fig. 1 incorporate uncertainties, errors, and randomness in the underlying algorithms. In addition, their behavior can be affected by initial conditions (e.g., the start point of the mission inside the indoor environment). To this end, the successful missions indicator M_s provides the ratio of completed missions over the number of times that the mission is repeated. This indicator reflects the effectiveness and robustness of our exploration strategy.

[10]Generic battery model, Mathworks, `https://bit.ly/3yYVXfn`
[11]ICUAS 2022 Competition Rulebook, `https://bit.ly/3NvV0iE`

TABLE II
RESULTS

Environment No.	Entry Point (x,y)	Target Location (x,y,z)	Performance Evaluation						
			E_c [m]	B_c [%]	R_e [m]	D_a [m]	T_t [s]	S_a [m/s]	M_s
$\mathcal{E}_1$	(-10.5,-5.5)	(4.5,7.5,2.97)	27.32±0.12	98.46±0.13	0.06±0.01	0.77±0.02	64±2.65	0.64±0.02	3/3
	(-10.5,-2.5)	(7.82,7.5,1.75)	**37.57±19.85**	**98.39±0.34**	0.04±0.03	**0.99±0.04**	**83±39**	0.66±0.23	3/3
	(-10.5,0)	(3.55,-7.5,2.43)	44.49±1.25	98.38±0.15	0.37±0.07	0.77±0.11	91.33±13.32	**0.71±0.06**	3/3
	(-10.5,2.5)	(12.5,0.18,3.42)	28.38±0.03	98.43±0.15	0.04±0.01	0.86±0.01	82±13.86	**0.58±0.01**	3/3
	(-10.5,5.5)	(6.35,-7.5,2.52)	38.23±0.68	98.31±0.07	**0.53±0.06**	0.86±0.05	97±2.65	0.58±0.04	3/3
$\mathcal{E}_2$	(-10.5,-5.5)	(4.5,7.5,2.97)	26.10±0.01	98.76±0.04	0.06±0.03	0.77±0.03	51±2	0.62±0.06	3/3
	(-10.5,-2.5)	(7.82,7.5,1.75)	**49.32±19.86**	**98.26±0.42**	0.03±0.03	**1.04±0.06**	**99.67±41.28**	**0.70±0.03**	3/3
	(-10.5,0)	(3.55,-7.5,2.43)	43.71±0.18	98.20±0.08	0.35±0.04	0.77±0.08	100.33±4.62	0.60±0.02	3/3
	(-10.5,2.5)	(12.5,0.18,3.42)	28.50±0.02	98.50±0.04	0.06±0.01	0.83±0.01	76.33±3.06	**0.55±0.01**	3/3
	(-10.5,5.5)	(6.35,-7.5,2.52)	37.99±0.08	98.53±0.39	**0.46±0.10**	0.83±0.05	94.67±4.73	0.57±0.02	3/3
$\mathcal{E}_3$	(-10.5,-5.5)	(4.5,7.5,2.97)	26.15±0.11	98.78±0.02	0.06±0.01	0.75±0.05	51±1	0.63±0.08	3/3
	(-10.5,-2.5)	(7.82,7.5,1.75)	**82.78±36.80**	**97.66±0.77**	0.03±0.01	**1.04±0.01**	**134.67±12.50**	**0.71±0.04**	3/3
	(-10.5,0)	(3.55,-7.5,2.43)	44.70±0.20	98.23±0.01	0.32±0.08	0.79±0.76	104.67±1.53	0.62±0.02	3/3
	(-10.5,2.5)	(12.5,0.18,3.42)	28.65±0.01	98.70±0.38	0.06±0.04	0.83±0.04	**69.67±19.66**	**0.54**	3/3
	(-10.5,5.5)	(6.35,-7.5,2.52)	39.56±2.35	98.25±0.02	**0.50±0.04**	0.75±0.12	102.33±3.79	0.60±0.02	3/3

B. Benchmark Results

In our study, we conducted a total of 45 simulation experiments, 3 runs for the same entry point and target location with 15 experiments in each of the three indoor environments. The aggregated results in terms of mean and standard deviation are tabulated in Table II for the aforementioned KPIs.

We consider $\mathcal{E}_1$, shown in Fig. 3 (top right marked as 1), with openly spaced obstructions. For the second entry point (-10.5,-2.5) and target location (7.82,7.5,1.75), we observe a higher exploration cost to complete the mission having traversed an average total distance, i.e., $E_c = 37.57\,\mathrm{m}$ with a standard deviation of ± 19.85, with remaining battery $B_c = 98.39\,\%$, and highest distance error, i.e., $D_a = 0.99$ standard deviation of ± 6.3 compared to other target locations.

The UAV missed to detect the target, i.e., the ARTag, in one of the runs in $\mathcal{E}_1$ because the target was placed very low to the ground, while the UAV was at a certain altitude not clearly visible in the FoV of the depth camera. However, once the UAV had entered in Zone 3, it was directed to traverse in a loop starting from the left wall provided with a set of 9 waypoints to stop and search the target, until either the target was detected or the battery depletes to 5%. However, in this case, we observed the total elapsed time $T_t = 83\,\mathrm{s}$ with a standard deviation of $\pm 39\,\mathrm{s}$ depicting the above stated behavior and with a higher delivery deviation of $D_a = 0.99\,\mathrm{m}$. Similarly, in $\mathcal{E}_2$ and $\mathcal{E}_3$ the same behavior was noted for the second entry point shown in bold.

Moreover, we observed in the fifth entry point (-10.5,5.5) and target location (6.35,-7.5,2.52) in all the three environments that the target reconstructed pose estimate was not accurate with a large offset of $R_e = 0.53\,\mathrm{m}$ due to the dark black texture of the wall. The average minimum and maximum speed noted was between $[0.54 - 0.71]\mathrm{m/s}$. Our findings indicate that the proposed UAV system lies within an acceptable threshold for UAV flights and can be rapidly deployed on a real-drone, which motivates further research on autonomous exploration strategies for indoor SAR real-life scenarios. A demo video of our solution in $\mathcal{E}_3$ preforming autonomous exploration, target detection and payload delivery is available online[12].

C. Lessons Learned

To put in perspective the complexity of the competition, our solution was one of the top-10 listed among 53 teams worldwide (in the simulation phase). We were ranked 6^{th} after the final evaluation[13] of 15 competing solutions who were successfully able to perform autonomous exploration, detect and launch the ball to the target from various entry points and target locations, i.e., the evaluation environment $\mathcal{E}_4$. The complexity of $\mathcal{E}_4$ can be visualized in Fig. 3 (right marked as 4), with a narrow opening, dead-ends, and a total of 11 obstructions compared to $\mathcal{E}_1 - \mathcal{E}_3$, as listed in Table I. The spider plot in Fig. 4 depicts the evaluation score, i.e., $ESi,\ i = 1, \ldots, 5$ for the five runs starting from different entry points and target locations tabulated in Table II. Although our solution was ranked 6^{th}, it performed better in $ES1$ and $ES2$ than the 5^{th} ranked team. We believe that the points for the mission complete were more biased towards total time duration which resulted in our lower points score. However, the robustness and effectiveness of our approach were evident from the performance evaluation in Table II.

The motivation for ICUAS 2022 UAV Competition was to further escalate research for indoor exploration and mapping for a single UAV. We developed an autonomous exploration and target detection solution in a much simpler and more effective manner for deployment in a real-life SAR mission. Mainly, a collision-avoidance approach navigation using only the laser scans, a target, i.e. ARTag detection, and a ballistic ball launch approach were articulated in this paper. There is certainly a trade-off among the various KPIs to select the best performing strategy for UAV exploration missions.

V. CONCLUSIONS

We put forward a perception-aware autonomous exploration approach aimed at performing target detection and

[12] `https://youtu.be/Z-trnvxgyOI`

[13] Simulation Phase (Final Ranking), `https://bit.ly/3z8jxqq`

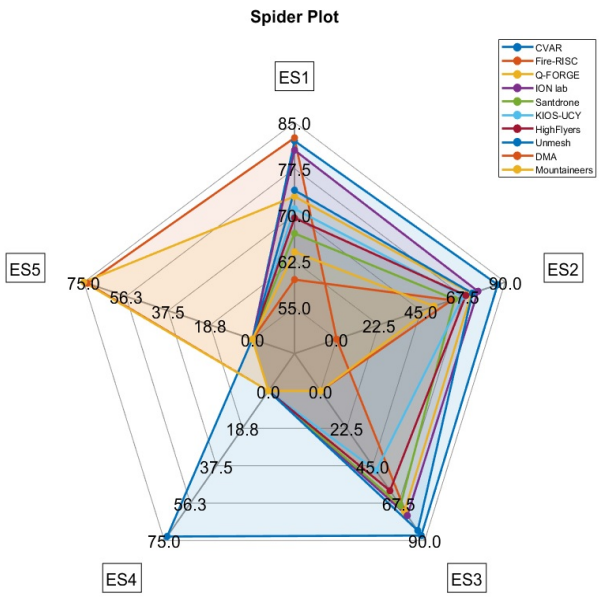

Fig. 4. Evaluation Score in $\mathcal{E}_4$.

collision avoidance. In particular, we aim to provide a generic solution for indoor exploration and mapping with varying levels of difficulty and challenge for fire-fighting missions on a common test-bed. An end-to-end baseline system architecture has been considered for developing our proposed approach. We showcase the potential of our approach via extensive simulations, aiming toward integrating and testing it into a real UAV platform. We also plan to investigate multi-UAV exploration through the frontier and sampling-based approaches toward finding the target. In addition, more challenging scenarios will be investigated, such as passing through narrow passageways, finding a new path from a dead-end, and considering static and dynamic obstacles.

REFERENCES

[1] A. Koubaa, E. T. Alotaibi, and S. S. Alqefari, "System, apparatus, and method for controlling unmanned aerial vehicles for search and rescue," Jul. 15 2021, uS Patent App. 16/740,042.

[2] A. Q. Nguyen, H. T. Nguyen, V. C. Tran, H. X. Pham, and J. Pestana, "A visual real-time fire detection using single shot multibox detector for uav-based fire surveillance," in *2020 IEEE Eighth International Conference on Communications and Electronics (ICCE)*, 2021, pp. 338–343.

[3] M. Ahsan, K. Abbas, A. Zahid, A. Farooq, and S. Mashhood Murtaza, "Modification of a toy helicopter into a highly cost effective, semi-autonomous, reconnaissance unmanned aerial vehicle," in *2012 International Conference of Robotics and Artificial Intelligence*, 2012, pp. 49–54.

[4] V. Spurny, V. Pritzl, V. Walter, M. Petrlik, T. Baca, P. Stepan, D. Zaitlik, and M. Saska, "Autonomous firefighting inside buildings by an unmanned aerial vehicle," *IEEE Access*, vol. 9, pp. 15 872–15 890, 2021.

[5] W. Hoshino, J. Seo, and Y. Yamazaki, "A study for detecting disaster victims using multi-copter drone with a thermographic camera and image object recognition by ssd," in *2021 IEEE/ASME International Conference on Advanced Intelligent Mechatronics (AIM)*, 2021, pp. 162–167.

[6] M. Wang and H. Voos, "An integrated teleoperation assistance system for collision avoidance of high-speed uavs in complex environments," in *2020 17th International Conference on Ubiquitous Robots (UR)*. IEEE, 2020, pp. 290–296.

[7] E. P. H. Alarcón, D. B. Ghavifekr, G. Baris, M. Mugnai, M. Satler, and C. A. Avizzano, "An efficient object-oriented exploration algorithm for unmanned aerial vehicles," in *2021 International Conference on Unmanned Aircraft Systems (ICUAS)*. IEEE, 2021, pp. 330–337.

[8] N. Chumuang, A. Farooq, M. Irfan, S. Aziz, and M. Qureshi, "Feature matching and deep learning models for attitude estimation on a micro-aerial vehicle," in *2022 International Conference on Cybernetics and Innovations (ICCI)*, 2022, pp. 1–6.

[9] B. Arbanas, F. Petric, A. Batinović, M. Polić, I. Vatavuk, L. Marković, M. Car, I. Hrabar, A. Ivanović, and S. Bogdan, "From erl to mbzirc: Development of an aerial-ground robotic team for search and rescue," in *Automation and Control - Theories and Applications*, P. E. P. Dadios, Ed. Rijeka: IntechOpen, 2021, ch. 2. [Online]. Available: https://doi.org/10.5772/intechopen.99210

[10] J. Quenzel, M. Splietker, D. Pavlichenko, D. Schleich, C. Lenz, M. Schwarz, M. Schreiber, M. Beul, and S. Behnke, "Autonomous fire fighting with a uav-ugv team at mbzirc 2020," in *2021 International Conference on Unmanned Aircraft Systems (ICUAS)*, 2021, pp. 934–941.

[11] E. Ackerman, "Robots conquer the underground: What darpa's subterranean challenge means for the future of autonomous robots," *IEEE Spectrum*, vol. 59, no. 5, pp. 30–37, 2022.

[12] M. Irfan and A. Farooq, "Auction-based task allocation scheme for dynamic coalition formations in limited robotic swarms with heterogeneous capabilities," in *2016 International Conference on Intelligent Systems Engineering (ICISE)*, 2016, pp. 210–215.

[13] A. Anastasiou, P. Kolios, C. Panayiotou, and K. Papadaki, "Swarm path planning for the deployment of drones in emergency response missions," in *2020 International Conference on Unmanned Aircraft Systems (ICUAS)*, 2020, pp. 456–465.

[14] M. Dharmadhikari, H. Nguyen, F. Mascarich, N. Khedekar, and K. Alexis, "Autonomous cave exploration using aerial robots," in *2021 International Conference on Unmanned Aircraft Systems (ICUAS)*, 2021, pp. 942–949.

[15] T. Elmokadem and A. V. Savkin, "A method for autonomous collision-free navigation of a quadrotor uav in unknown tunnel-like environments," *Robotica*, vol. 40, no. 4, p. 835–861, 2022.

[16] D. Shim, H. Chung, H. J. Kim, and S. Sastry, "Autonomous exploration in unknown urban environments for unmanned aerial vehicles," in *AIAA Guidance, Navigation, and Control Conference and Exhibit*, 2005, p. 6478.

[17] S. Shen, N. Michael, and V. Kumar, "Autonomous multi-floor indoor navigation with a computationally constrained mav," in *2011 IEEE International Conference on Robotics and Automation*. IEEE, 2011, pp. 20–25.

[18] A. Farooq, C. Laoudias, P. S. Kolios, and T. Theocharides, "Quantitative and qualitative assessment of indoor exploration algorithms for autonomous uavs," in *2022 International Conference on Unmanned Aircraft Systems (ICUAS)*, 2022. [Online]. Available: https://doi.org/10.48550/arXiv.2205.13801

[19] G. Grisetti, C. Stachniss, and W. Burgard, "Improved techniques for grid mapping with rao-blackwellized particle filters," *IEEE transactions on Robotics*, vol. 23, no. 1, pp. 34–46, 2007.

[20] Q.-C. Pham, "A general, fast, and robust implementation of the time-optimal path parameterization algorithm," *IEEE Transactions on Robotics*, vol. 30, no. 6, pp. 1533–1540, 2014.

[21] P. Jin, P. Matikainen, and S. S. Srinivasa, "Sensor fusion for fiducial tags: Highly robust pose estimation from single frame rgbd," in *2017 IEEE/RSJ International Conference on Intelligent Robots and Systems (IROS)*. IEEE, 2017, pp. 5770–5776.

[22] A. Barišić, F. Petric, and S. Bogdan, "Brain over brawn–using a stereo camera to detect, track and intercept a faster uav by reconstructing its trajectory," *arXiv preprint arXiv:2107.00962*, 2021.

[23] Z. Yan, L. Fabresse, J. Laval, and N. Bouraqadi, "Metrics for performance benchmarking of multi-robot exploration," in *2015 IEEE/RSJ International Conference on Intelligent Robots and Systems (IROS)*, 2015, pp. 3407–3414.